OL | Organic Letters

pubs.acs.org/OrgLett

Letter

Effect of Twisting on the Capture and Release of Singlet Oxygen by Tethered Twisted Acenes

Anjan Bedi, Amit Manor Armon, and Ori Gidron*

Cite This: *Org. Lett.* 2020, 22, 7809–7813

Read Online

ACCESS | Metrics & More | Article Recommendations | Supporting Information

ABSTRACT: The use of polyaromatic hydrocarbons to capture and release singlet oxygen is of considerable importance in materials chemistry, synthesis, and photodynamic therapy. Here we studied the ability of a series of tethered twistacenes, possessing different degrees of backbone twist, to capture and release singlet oxygen via the reversible Diels–Alder reaction. When the twistacene acts as both a sensitizer and a diene, the photo-oxidation rate depends on the extinction coefficient of the irradiation wavelength. However, when the twistacenes function solely as a diene, the rate of photo-oxidation increases with increasing twist. The rate of the reverse reaction, the singlet oxygen release, also increases with increasing twist. The calculated transition state energy decreases with increasing twist, which can explain the observed trend. The presence of the tether significantly increases the reversibility of the reaction, which can proceed in repeated forward and reverse cycles in very high yield under mild conditions, as required for molecular switches.

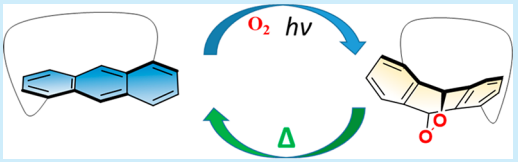

Singlet oxygen ($^1O_2$) is widely used in synthesis and in biological and materials science applications.[1,2] Acenes can undergo oxygenation with $^1O_2$ to yield endoperoxides, which, in turn, can release $^1O_2$ and parent acene. This reversible capture and release of $^1O_2$ has been applied in lithographic applications, luminescent $^1O_2$-response polymer design, oxygen storage, and molecular rotors.[3−8] Consequently, the ability to predict acene reactivity toward oxygenation and the degree of reversibility of that reaction are of great importance. However, the factors that govern reactivity with respect to both the capture and release of $^1O_2$ from polyaromatic hydrocarbons (PAHs) are not well understood, making it difficult to predict and design suitable candidates for this purpose.[9,10]

Recently, we attached an end-to-end diagonal tether to the conjugated backbones of phenyl-substituted anthracenes to produce a new family of twistacenes, **Ant-C*n***.[11] We were thus able to produce helically locked conformations of stable *M* and *P* **Ant-C*n*** enantiomers in which the tether prevents the formation of a racemized mixture (by preventing back and forth flipping around the backbone), and the length of the tether controls the degree of backbone twist while minimizing the effect of side groups. We found that the twist angle strongly and systematically affects several important properties. Specifically, the larger the twist angle is in **Ant-C*n***, the lower the fluorescence quantum efficiency ($\varnothing_f$) and half-life time (τ_f), the smaller the optical band gap, the greater the Cotton effect, and the larger the absorption anisotropy factor.[12,13] However, the effect of acene twisting on the chemical reactivity remains an open question.[14] Previously, the reactivity of nonplanar PAHs was studied with respect to the effect of strain. For example, Bodwell's group demonstrated that the reactivity of bent pyranophanes increases with increasing strain.[15,16] Houk's group calculated the Diels–Alder reactivity of dienophiles and concluded that strained dienophiles are more reactive as a result of strain release.[17]

Here we studied the effect of acene twist on $^1O_2$ capture and release by enantiopure members of the **Ant-C*n*** series (Scheme 1). We found that when **Ant-C*n*** is both the sensitizer and the diene, the rate of oxygenation depends on the wavelength of irradiation resulting from differences in extinction coefficients. When **Ant-C*n*** is not involved in oxygen sensitization, the rate of oxygenation increases with increasing twist. The rate for the release of singlet oxygen shows the same trend and

Scheme 1. Reversible Capture and Release of $^1O_2$ by Ant-C*n*[a]

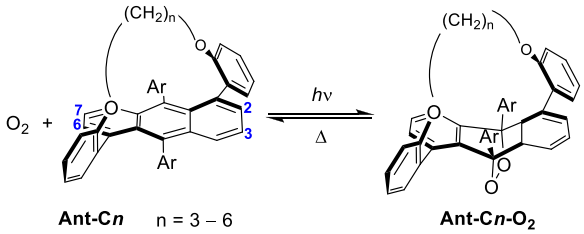

[a]Ar = 3,5-bis(trifluoromethyl)phenyl.

Received: August 10, 2020
Published: September 23, 2020

https://dx.doi.org/10.1021/acs.orglett.0c02666
Org. Lett. 2020, 22, 7809–7813

systematically increases with increasing twist. Density functional theory (DFT) calculations support these findings, as the activation parameters decrease with twist. Switching experiments demonstrated that tethering greatly improves the stability by reducing side reactions.

Chloroform solutions of enantiopure **Ant-C*n*** form were subjected to 427 or 365 nm irradiation at room temperature. The reaction was followed by UV−vis spectroscopy, with the formation of an absorption band in the 280−300 nm region and the disappearance of the absorption band in the 330−450 nm and 260 nm regions (as exemplified by **Ant-C4** in Figure 1a). The irradiation products were isolated using column

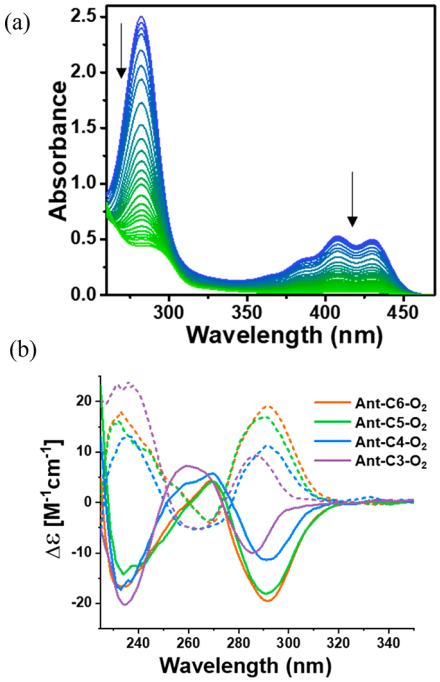

Figure 1. Absorbance and ECD spectra. (a) Absorbance spectra of the gradual photo-oxidation of **Ant-C4** (blue) irradiated at 427 nm to form **Ant−C4-O$_2$** (green) showing the formation and disappearance (downward arrows) of bands during photo-oxidation. (b) ECD spectra of the **Ant-C*n*-O$_2$** series. Dashed line represents the oxidized product of ***P*-Ant-C*n*** and solid line represents the oxidized product of ***M*-Ant-C*n***.

chromatography and characterized using ^{1}H and ^{13}C NMR and mass spectrometry. The NMR spectroscopy indicates that the irradiation products, **Ant-C*n*-O$_2$**, retain the expected C_2 symmetry, with free rotation of the bistrifluoromethylphenyl rings on the NMR time scale. The only significant difference in **Ant-C*n*-O$_2$** compared with **Ant-C*n*** is the upfield shift of the carbon at the 9,10-position of anthracene from 135 to 84 ppm as it adopts a tetrahedral configuration. (See the SI.)

The cycloadducts were recrystallized in hexane/chloroform to yield white needles. The X-ray structure of **Ant−C5-O$_2$** revealed a dihedral angle (between the terminal carbons 2−3−6−7, as depicted in Scheme 1) of 16° compared with 7° for its nontethered analog **Ant-Open-O$_2$**. Thus the tether contributes 9° of the observed twist, whereas steric hindrance can account for the remaining 7° (Figure 2). It is noteworthy that whereas **Ant−C5-O$_2$** was crystallized from its racemic mixture, the crystal consists of only one enantiomer, and hence it crystallizes as a conglomerate, as opposed to the crystal structures of all **Ant-C*n***, which were found to be racemates.[11]

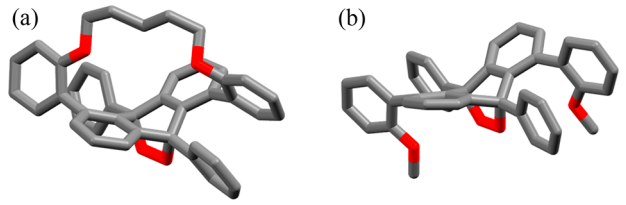

Figure 2. X-ray structure of (a) **Ant-C5-O$_2$** and (b) **Ant-Open-O$_2$**. Hydrogens and trifluoromethyl groups are omitted for clarity.

P- and *M*-enantiomers of **Ant-C*n*-O$_2$**, which were obtained from the corresponding enantiomers of **Ant-C*n***, were studied by electronic circular dichroism (ECD) spectroscopy. For the lowest energy transition, the ECD spectra of **Ant-C*n*-O$_2$** (Figure 1b) display the opposite trend to that previously observed for **Ant-C*n***,[13] undergoing a hypsochromic shift and decreasing in intensity as the tether shortens.

To study the effect of twisting on reactivity, the samples were irradiated at two different wavelengths: 427 nm, which accounts for the $\pi-\pi^*$ transition and for which the extinction coefficient increases with twist (a difference of 70% from **Ant-C6** to **Ant-C3**), and 365 nm, in which the extinction coefficients for **Ant-C5**, **-C4**, and **-C3** have similar values (a difference of 5% between **Ant-C5** and **Ant-C3**, while **Ant-C6** is 13% higher than **Ant-C3**; Table S1). As portrayed in Figure 3,

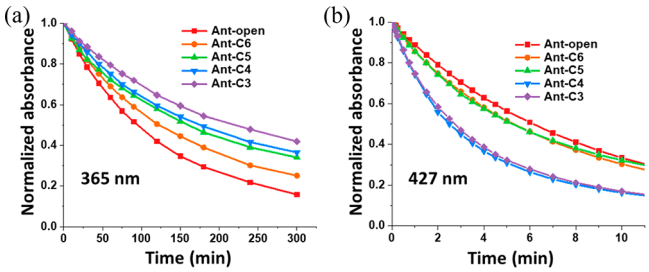

Figure 3. Change in normalized absorbance of **Ant-C*n*** at the $\pi-\pi^*$ transition upon irradiation at (a) 365 and (b) 427 nm.

the rate of photo-oxidation clearly depends on the wavelength chosen: The rate increases with the twist angle at 427 nm, whereas it decreases with the twist angle at 365 nm. Overall, when **Ant-C*n*** serves as both the sensitizer and the diene, the trend in reactivity can be controlled by the chosen irradiation wavelength.

Several factors can potentially account for the slower rate observed with increased anthracene twisting when irradiated at 365 nm. Because the anthracene serves as both the sensitizer and the diene, the generation of singlet oxygen also needs to be taken into account. To separate between the roles of **Ant-C*n*** as a photosensitizer and a diene, the reactions were studied with a catalytic amount of methylene blue (MB) sensitizer under irradiation at 617 nm, at which **Ant-C*n*** does not absorb (Figure S47). We found that the reaction rate increases with increasing twist. This indicates that the trend observed when **Ant-C*n*** serves as both a sensitizer and a diene strongly depends on its role as a sensitizer, and the rate-determining step involves the oxygen sensitization process rather than the cycloaddition.[18,19]

Previous studies have shown that anthracene can react with oxygen in two competing mechanisms after the first excitation to the S_1 level: a concerted mechanism, involving an intersystem crossing (ISC) pathway to form T_1, which reacts

https://dx.doi.org/10.1021/acs.orglett.0c02666
Org. Lett. 2020, 22, 7809−7813

with $^3O_2$ to form $^1O_2$, and an electron transfer to $^3O_2$ to form radical $O_2^{\bullet-}$ (Scheme 2).[9,10,18,20] We have previously

Scheme 2. Possible Pathways for Oxygen Sensitization of Ant-C*n*

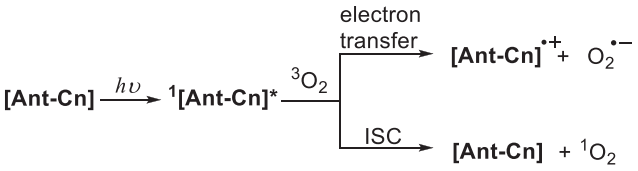

demonstrated that as twisting increases, the rate of ISC to the triplet state also increases.[21] Therefore, it is expected that as the twisting increases, the mechanism that involves ISC will become more dominant. When using MB as the sensitizer, the faster reaction rate with twisting can be explained by the calculated lower energy for the transition state of twisted **Ant-C3** compared with less-twisted **Ant-C6**, as detailed later.

When heated in the dark, **Ant-C*n*-O$_2$** undergoes cycloreversion, resulting in **Ant-C*n*** and singlet oxygen. Switching experiments performed at −5 °C for photo-oxidation and 110 °C for cycloreversion demonstrated that after 15 cycles of such irradiation/heating, >70% of the tethered twistacene remains, indicating its potential as a reversible switch with an average yield of 98% per capture/release cycle (Figure 4, purple). This

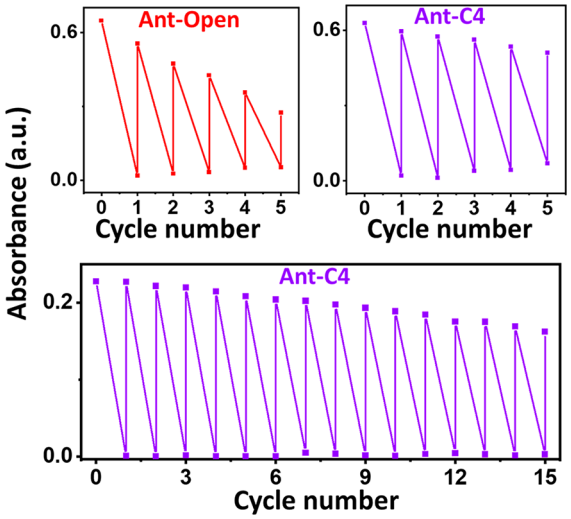

Figure 4. Top: Switching experiment for **Ant-C4/Ant−C4-O$_2$** and **Ant-Open/Ant-Open-O$_2$** in 1,1,2,2-tetrachloroethane under irradiation at 427 nm at −5 °C for photo-oxidation and upon heating to 135 °C for cycloreversion. Absorbance was measured at 430 and 406 nm for **Ant-Open** and **Ant-C4**, respectively. Bottom: 15 cycles of the switching experiment for **Ant-C4/Ant−C4-O$_2$** heating to 110 °C.

is in contrast with untethered anthracene, which shows fast decomposition and a slow rate of cycloreversion at 135 °C (Figure 4, red). Unlike tethered acenes, the capture and release of $^1O_2$ by **Ant-Open** result in quick decomposition, with only 42% of the compound remaining after five cycles compared with 81% of **Ant-C4**. The presence of the tether protects the anthracene from overoxidation; therefore, tethered anthracenes are ideal agents for the capture and release of oxygen, functioning as switches.

The NMR kinetic study revealed that the retro Diels−Alder reaction rate increases with increasing twist. For example, at 80 °C, the rate increases by more than an order of magnitude from 6.9 × 10^{-5} s^{-1} for **Ant-C6** to 1.1 × 10^{-3} s^{-1} for **Ant-C4** (Table S2). We investigated the activation parameters for the retro Diels−Alder reaction by expressing the VT-NMR data in Eyring plots. As can be observed in Figure 5a, $\Delta G^{\ddagger}$ decreases

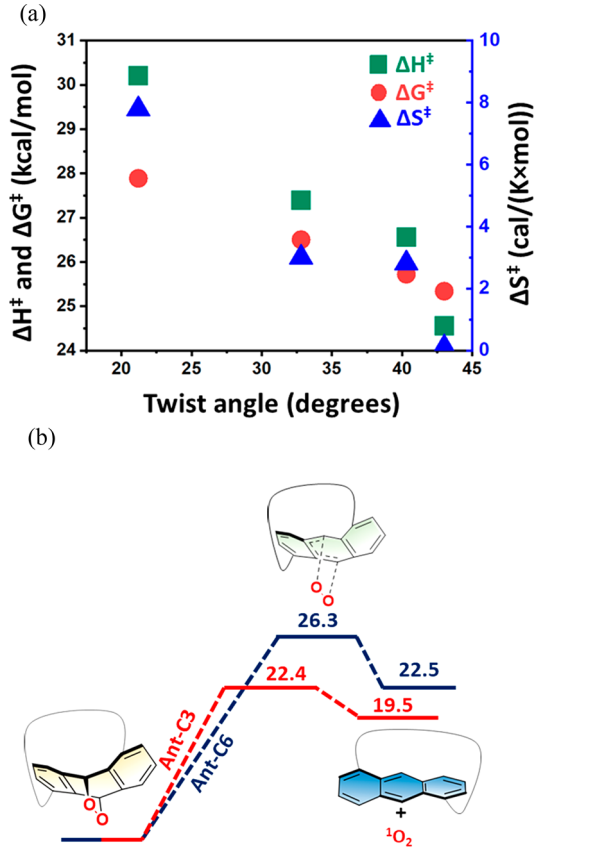

Figure 5. (a) Experimental kinetic parameters of the thermal retro Diels−Alder reaction for different tether lengths. (b) Calculated (B3LYP/6-31G(d), in kcal/mol) $\Delta G^{\ddagger}$ for retro Diels−Alder of **Ant-C3** (red) and **Ant-C6** (blue).

from 27.9 kcal/mol for **Ant-C6** to 25.3 kcal/mol for **Ant-C3**. This primarily stems from the decrease in the heat of activation ($\Delta H^{\ddagger}$), despite a decrease in the activation entropy ($\Delta S^{\ddagger}$). The retro Diels−Alder reaction was also studied using DFT calculations at the B3LYP/6-31G(d) level of theory. The trend in the free energy of activation is in agreement with the experimental values, with $\Delta G^{\ddagger}$ decreasing from 26.3 kcal/mol for **Ant-C6** to 22.4 kcal/mol for **Ant-C3** (Figure 5b).

The HOMO levels of the twistacenes remain almost constant with twist.[11] However, the examination of the HOMO coefficients of the central carbons (in the 9- and 10-positions) in the transition states of **Ant-C6** and **Ant-C3** reveals an increase of 17% in the sum of the atomic orbital coefficients for **Ant-C3** compared with **Ant-C6** (Table S11 and Figure S59).[22] This difference can account for the stabilization of the transition state and, consequently, for the faster reaction rate observed with increasing twist for both cycloaddition and cycloreversion. We note that strain release can also account for the observed reactivity: Because both twisted **Ant-C*n*-O$_2$** and **Ant-C*n*** have higher energies as the tether shortens, the activation energy should be smaller, making both the Diels−

https://dx.doi.org/10.1021/acs.orglett.0c02666
Org. Lett. 2020, 22, 7809−7813

Alder and the retro Diels–Alder reactions faster with increasing acene twist.

In summary, we studied the reactivity of twisted anthracene toward photo-oxidation and retro Diels–Alder reactions. We found that reactivity systematically depends on the degree of twisting. The rate of photo-oxidation increases with increasing twist when the twistacene acts as a diene and shows dependency on the extinction coefficient when the twistacene acts as both the diene and the sensitizer. The rate of singlet oxygen release by the retro Diels–Alder reaction follows a first-order kinetics and increases with increasing twist. The calculated activation parameters are in line with the experimental values, and the calculated $\Delta G^{\ddagger}$ for **Ant-C3** is lower by 3.9 kcal/mol compared with **Ant-C6**. The reaction, which proceeds under mild conditions, is reversible, with an average 98% yield per capture/release cycle, indicating that tethered twistacenes can serve as excellent sources of singlet oxygen.

■ ASSOCIATED CONTENT

Supporting Information

The Supporting Information is available free of charge at https://pubs.acs.org/doi/10.1021/acs.orglett.0c02666.

Experimental procedures, spectral data, X-ray structural data, details of electrochemical measurements, and computational details (PDF)

Cartesian coordinates for optimization (TXT)

Accession Codes

CCDC 1982853 and 1989525 contain the supplementary crystallographic data for this paper. These data can be obtained free of charge via www.ccdc.cam.ac.uk/data_request/cif, or by emailing data_request@ccdc.cam.ac.uk, or by contacting The Cambridge Crystallographic Data Centre, 12 Union Road, Cambridge CB2 1EZ, UK; fax: +44 1223 336033.

■ AUTHOR INFORMATION

Corresponding Author

Ori Gidron − *Institute of Chemistry, The Hebrew University of Jerusalem, Jerusalem 91904, Israel;* orcid.org/0000-0002-7037-0563; Email: ori.gidron@mail.huji.ac.il

Authors

Anjan Bedi − *Institute of Chemistry, The Hebrew University of Jerusalem, Jerusalem 91904, Israel;* orcid.org/0000-0001-6418-4409

Amit Manor Armon − *Institute of Chemistry, The Hebrew University of Jerusalem, Jerusalem 91904, Israel;* orcid.org/0000-0002-6866-6701

Complete contact information is available at: https://pubs.acs.org/10.1021/acs.orglett.0c02666

Notes

The authors declare no competing financial interest.

■ ACKNOWLEDGMENTS

This research was supported by the European Research Council (ERC) under the European Union's Horizon 2020 research and innovation program (grant agreement no. 850836, ERC Starting Grant "PolyHelix"). We thank Dr. Benny Bogoslavsky (The Hebrew University of Jerusalem, Israel) for X-ray structure determination.

■ REFERENCES

(1) Ushakov, D. B.; Gilmore, K.; Kopetzki, D.; McQuade, D. T.; Seeberger, P. H. Continuous-Flow Oxidative Cyanation of Primary and Secondary Amines Using Singlet Oxygen. *Angew. Chem., Int. Ed.* **2014**, *53*, 557–561.

(2) DeRosa, M. C.; Crutchley, R. J. Photosensitized singlet oxygen and its applications. *Coord. Chem. Rev.* **2002**, *233–234*, 351–371.

(3) Zehm, D.; Fudickar, W.; Linker, T. Molecular Switches Flipped by Oxygen. *Angew. Chem., Int. Ed.* **2007**, *46*, 7689–7692.

(4) He, Y.-Q.; Fudickar, W.; Tang, J.-H.; Wang, H.; Li, X.; Han, J.; Wang, Z.; Liu, M.; Zhong, Y.-W.; Linker, T.; Stang, P. J. Capture and Release of Singlet Oxygen in Coordination-Driven Self-Assembled Organoplatinum(II) Metallacycles. *J. Am. Chem. Soc.* **2020**, *142*, 2601–2608.

(5) Fudickar, W.; Linker, T. Release of Singlet Oxygen from Organic Peroxides under Mild Conditions. *ChemPhotoChem.* **2018**, *2*, 548–558.

(6) Fudickar, W.; Linker, T. Novel Anthracene Materials for Applications in Lithography and Reversible Photoswitching by Light and Air. *Langmuir* **2010**, *26*, 4421–4428.

(7) Fudickar, W.; Linker, T. Photoimaging with Singlet Oxygen at the Solid–Air Interface. *Langmuir* **2009**, *25*, 9797–9803.

(8) Fudickar, W.; Fery, A.; Linker, T. Reversible Light and Air-Driven Lithography by Singlet Oxygen. *J. Am. Chem. Soc.* **2005**, *127*, 9386–9387.

(9) Aubry, J. M.; Pierlot, C.; Rigaudy, J.; Schmidt, R. Reversible binding of oxygen to aromatic compounds. *Acc. Chem. Res.* **2003**, *36*, 668–675.

(10) Schweitzer, C.; Schmidt, R. Physical mechanisms of generation and deactivation of singlet oxygen. *Chem. Rev.* **2003**, *103*, 1685–757.

(11) Bedi, A.; Shimon, L. J. W.; Gidron, O. Helically Locked Tethered Twistacenes. *J. Am. Chem. Soc.* **2018**, *140*, 8086–8090.

(12) Bedi, A.; Carmieli, R.; Gidron, O. Radical cations of twisted acenes: chiroptical properties and spin delocalization. *Chem. Commun.* **2019**, *55*, 6022–6025.

(13) Bedi, A.; Gidron, O. Chiroptical Properties of Twisted Acenes: Experimental and Computational Study. *Chem. - Eur. J.* **2019**, *25*, 3279–3285.

(14) Bedi, A.; Gidron, O. The Consequences of Twisting Nanocarbons: Lessons from Tethered Twisted Acenes. *Acc. Chem. Res.* **2019**, *52*, 2482–2490.

(15) Bodwell, G. J.; Fleming, J. J.; Mannion, M. R.; Miller, D. O. Nonplanar Aromatic Compounds. 3. A Proposed New Strategy for the Synthesis of Buckybowls. Synthesis, Structure and Reactions of [7]-, [8]- and [9](2,7)Pyrenophanes. *J. Org. Chem.* **2000**, *65*, 5360–5370.

(16) Bodwell, G. J.; Bridson, J. N.; Houghton, T. J.; Kennedy, J. W. J.; Mannion, M. R. 1,7-Dioxa[7](2,7)pyrenophane: The Pyrene Moiety Is More Bent than That of C70. *Chem. - Eur. J.* **1999**, *5*, 1823–1827.

(17) Liu, F.; Liang, Y.; Houk, K. N. Theoretical Elucidation of the Origins of Substituent and Strain Effects on the Rates of Diels–Alder Reactions of 1,2,4,5-Tetrazines. *J. Am. Chem. Soc.* **2014**, *136*, 11483–11493.

(18) Reddy, A. R.; Bendikov, M. Diels–Alder reaction of acenes with singlet and triplet oxygen − theoretical study of two-state reactivity. *Chem. Commun.* **2006**, 1179–1181.

(19) Fudickar, W.; Linker, T. Remote substituent effects on the photooxygenation of 9,10-diarylanthracenes: strong evidence for polar intermediates. *Chem. Commun.* **2008**, 1771–1773.

(20) Fudickar, W.; Linker, T. Why Triple Bonds Protect Acenes from Oxidation and Decomposition. *J. Am. Chem. Soc.* **2012**, *134*, 15071–15082.

(21) Tait, C. E.; Bedi, A.; Gidron, O.; Behrends, J. Photoexcited triplet states of twisted acenes investigated by Electron Paramagnetic Resonance. *Phys. Chem. Chem. Phys.* **2019**, *21*, 21588–21595.

(22) Tsuneda, T. Chemical reaction analyses based on orbitals and orbital energies. *Int. J. Quantum Chem.* **2015**, *115*, 270−282.

https://dx.doi.org/10.1021/acs.orglett.0c02666
Org. Lett. 2020, 22, 7809−7813